ISSN 0029-3865

CBPF-NF-061/85

MAGNETIC PROPERTIES OF TETRATAENITE-RICH METEORITES II

by

T. Nagata*, M. Funaki* and J. Danon

Centro Brasileiro de Pesquisas Físicas - CNPq/CBPF
Rua Dr. Xavier Sigaud, 150
22290 - Rio de Janeiro, RJ - Brasil

*National Institute of Polar Research, Tokyo

Abstract

Magnetic hysteresis and thermomagnetic characteristics of St. Séverin (LL_6), Appley Bridge (LL_6) and Tuxtuac (LL_5) chondrites, which contain tetrataenite in their metallic components, are measured and analyzed in comparison with another tetrataenite-rich chondrite, Yamato 74160.

The magnetic properties of tetrataenite-rich meteorites are characterized by (a) high magnetic coercive force (H_C)which amounts to 520 Oe for St. Séverin and 160 Oe for Appley Bridge, (b) essential flatness up to about 500°C and then a sharp irreversible drop down to Curie point of the first-run heating thermomagnetic curve. Both characteristic features are broken down to the ordinary features of disordered taenite by a breakdown of tetrataenite structure at elevated temperatures beyond the order-disorder transition temperature.

The natural remanent magnetization (NRM) of tetrataenite-rich meteorites is extremely stable against AF-demagnetization and other magnetic disturbances because of the high magnetic coercivity of tetrataenite. The breakdown processes of ordered tetrataenite structure by heat treatments are experimentally persued for the purpose of research of a possible formation process of tetrataenite phase in meteorites.

Key-words: Magnetism; Tetrataenite; Meteorites.

1 INTRODUCTION

In previous papers (Nagata and Funaki 1982, 1983), magnetic properties of 74160 LL_7 chondrite, Allan Hills 77260 L_3 chondrite. St. Séverein LL_6 chondrite and Allan Hills 77219 mesosiderite, which contain the tetrataenite phase in their metallic components, have been reported. As the magnetic coercivity of tetrataenite is extremely high because of its large magnetic anisotiopy owing to its tetragonal crystal structure, the natural remanent magnetization (NRM) of tetrataenite-rich meteorites is exclusively stable against AF-demagnetizations or simillar disturbances. It seems likely therefore that tetrataenite-rich meteorites are uniquely important in paleomagnetic studies of the primordial solar system.

Clarke and Scott (1980) pointed out that they have optically detected the tetrataenite phase in 15 H chondrites, 8 L chondrites, 9 LL chondrites, 18 mesosiderites, 2 pallasites, 6 ions and a diogenite. Among these meteorites which are optically proved to contain the tetrataenite phase, Allen Hills 77219 mesosiderite (Nagata and Funaki, 1983), Estherville mesosiderite and Appley Bridge LL_6 chondrite (Wasilewski, 1982) are examined magnetically also to detect presence of tetrataenite in them. The tetrataenite phase in Yamato 74160 and Allen Hills 77260 chondrites has been detected on the basis of its optical anisotropy in addition to its characteristic chemical composition of 50%Fe50%Ni in atomic ratio (Nagata and Funaki 1982, 1983),

while that in St. Séverin chondrite on the basis of Mössbauer spectra (Danon et al., 1979), before characteristic behaviours of magnetic properties caused by the presence of tetrataenite phase in these meteorites are magnetically examined.

Characteristic magnetic behaviours of tetrataenite phase observed so far in these tetrataenite-rich meteorites may be summarized by two main features, namely (a) a constancy of saturation magnetization intensity with a very small decreasing rate with increasing temperature up to about 450°C, which is irreversibly broken down by heating above Curie point, and (b) an unusurally high magnetic coercivity which also is broken down to a low coercivity state of the disordered taenite caused by a breakdown of the anisotropic ordered structure by heating above Curie point. It appears, however, that the magnetic behaviours of tetrataenite phase in meteorites are fairly complicated owing to coexistence of disordered taenites and kamacites of various Ni contents, which are in close contact with the tetrataenite phase in individual metallic grains (e.g. Nagata and Funaki, 1982).

Since the formation and breakdown processes of tetrataenite phase and necessary conditions for its equilibrium state in meteorites are not fully clarified yet, descriptions in detail of mineralogical and magnetic properties of as many tetrataenite-rich meteorites as available will be still reqeuired in the next step of studies. In the present work, magnetic properties of St. Séverin (LL_6), Appley Bridge (LL_6) and Tuxtuac (LL_5) tetrataenite-rich chondrites will be examined with

reference to their metallic compositions which are estimated by Mössbauer spectral analyses and other methods. In particular, St. Séverin chondrite is magnetically examined in fair detail, because only metallic grains of St. Séveren were magnetically examined in the previous work. In the present report, bulk specimen, matrix, clast, metallic grains and apparently pure tetrataenite phase specimens extracted from whole metallic grains of St. Séverin chondrite are separately examined.

2 ST. SÉVERIN LL_6 CHONDRITE

2.1. Composition and structure of metallic component

Results of Mössbauer spectral analysis of metallic component and an almost pure tetrataenite phase extracted from the metal of St. Séverin are represented by relative abundances of tetrataenite (TT), disordered taenite of less than 30% in Ni content which is paramagnetic at room temperature (PT) and kamacite (K) as

(TT):(PT):(K)=51:9.5:39.5 (in wt%)

for the whole metal, and

(TT):(PT):(K)=74:26: 0 (in wt%)

for almost pure tetrataenite phase.

Chemical compositions of opaque minerals in St. Séverin are newly measured with the aid of an electron microprobe analyzer,

results being summarized in Table 1, where chemical compositions of taenite, kamacite and troilite are separately summarized. As shown in Table 1, the average composition of taenite phase is given by (55.92±2.4) wt% Fe, (44.39±1.8) wt% Ni and (0.78±0.31) wt% Co, which are considerably deviated from the chemical composition of stoichiometric tetrataenite, i.e. 48.76 wt% Fe, 51.24 wt% Ni. Danon et al. (1979 a) have already reported that grain sizes of the ordered tetrataenite phase in paramagnetic matrix of Ni-poor taenite in St. Séverin metallic components are ranged mostly from 0.15μm to 0.3μm. It seems likely therefore that the chemical compositions of taenite phase obtained by the electron microprobe analyzer of 3μm in beam diameter represent, is most cases, average values of chemical compositions of the fine tetrataenite grains and the surrounding Ni-poor taenite. Actually, scanning surveys of low accurancy of the chemical composition of taenite surface of St. Séverin metallic grains have occasionally shown a group of composition such as (50.0% Fe, 52.3% Ni, 0.4% Co) or (45.9%Fe, 53.1%Ni, 3.1%Co) and another group of composition such as (63.3% Fe, 33.9% Ni, 0.0% Co), or (62.6% Fe, 34.3% Ni, 1.2% Co). The former group may represent a tetrataenite-rich spot, while the latter group a low-Ni taenite matrix spot.

The average chemical composition of kamacite phase in St. Séverin is given by (91.55±1.06)wt%Fe, (5.16±0.04)wt%Ni, (3.57±0.40)wt%Cc. The chemical composition of kamacite phase is much more homogeneous than that of taenite phase, as expected.

2.2. Basic magnetic properties.

Basic magnetic properties which characterize ferromagnetic hysteresis curves are measured at room temperature and at liquid He temperature for the bulk specimen, matrix, clast, metallic grains and apparent tetrataenite phase extracted from the metals of St. Séverin. The magnetic measurements are carried out before the meteorite samples are heated up to elevated temperatures beyond their Curie point and after the heating procedure. Saturation magnetization (I_S), saturated isothermal remanent magnetization (I_R), coercive force (H_C) and remenence coercive force (H_{RC}) are the measured basic ferromagnetic parameters of these samples, as summarized in Table 2.

It is noted first in Table 2 that both H_C and I_R of all samples of St. Séverin are much reduced after heating in comparison with their initial values before the heating, indicating that the original ordered tetrataenite structure is broken down to the disorederd taenite structure by the heating procedure. It will be further noted that ratios

$\{I_R(\text{Before heating})/I_R(\text{After heating})\}$,
$\{H_C(\text{Before heating})/H_C(\text{After heating})\}$ and
$\{H_{RC}(\text{Before heating})/H_{RC}(\text{After heating})\}$ observed at room temperature are particularly large for metals and extracted tetrataenite phase metals in comparison with those for bulk, matrix and clast samples. This result may suggest that the

breakdown phenomenon of ordered tetrataenite structure in bulk, matrix and clast samples by heating is associated with some chemical and structural reactions between tetrataenite phase and non-tetrataenite components at elevated temperatures, resulting thus in relaxing the sharp breakdown phenomenon of the magnetically coercive tetrataenite structure at elevated tempratures. As already discussed (Nagata and Funaki, 1982), magnetic coercive force (H_C) of tetrataenite crystal itself along its easy magnetization axis is theoretically estimated to be about 4.9×10^3 Oe and the observed values of H_C smaller than 10^3 Oe of all samples shown in Table 2 are due to coexistence of ferromagnetic component(s) of much lower coercivity.

It may have to be remarked that matrix and clast in Table 2 are not those which are extracted from the same bulk sample given in the same table. Since the distribution of metallic grains in St. Séverin is fairly heterogeneous, the I_S values of its bulk, matrix and clast specimens can be different from one another by factor 2. For example, the ferromagnetic hystresis parameters at room temperature of a bulk sample of St. Séverin examined in a preliminary study (Nagata and Fukui, 1982) are given by I_S=4.07 emu/g, I_R=0.54 emu/g, H_C=500 Oe and H_{RC}=1900 Oe. In regard to Table 2, therefore, ferromagnetic parameters related to magnetic coercivity such as I_R/I_S, H_C and H_{RC} will be the main interest in the present study.

2.3. Thermomagnetic curve characteristics.

The first-run thermomagnetic curves of a bulk sample of St. Séverin in a temperature range between -269°C and 850°C in a magnetic field of 10 kOe are shown in Fig.1. The cooling thermomagnetic curve of the second-run is approximaly same as the first-run cooling thermomagnetic curve, though the second-run heating thermomagnetic curve also has a kamacite magnetization component which is represented by $\alpha \rightarrow \gamma$ transition point of kamacite at 780°C.

Fig 2 (a),(b),(c) and (d) illustrate thermomagnetic curves of matrix, clast, whole metallic component and apparent tetrataenite phase extracted from metallic grains respectively, all in a magnetic field of 10 kOe for a temperature range between 20°C and 820°C. In the first-run heating thermomagnetic curves of all bluk, matrix, clast, metal and extracted tetrataenite of St. Séverin, a sharp magnetic transition takes place at 560 ~ 565°C, which may correspond to Curie point (Θ_C) of taenite of 56 wt% Ni. In the first-run heating thermomagnetic curves of bulk, matrix, clast and whole metal, a magnetic transition at 780~785°C corresponds to the $\alpha \rightarrow \gamma$ transition point ($\Theta^*_{\alpha \rightarrow \gamma}$) of kamacite containing a small amount of cobalt. In the first-run cooling thermomagnetic curves of bulk, matrix and clast, the $\gamma \rightarrow \alpha$ transition point ($\Theta^*_{\gamma \rightarrow \alpha}$) of kamacite phase is not clearly detected, but the $\Theta^*_{\gamma \rightarrow \alpha}$ point of kamacite is clearly observable at 665°C in both first- and second-run cooling curves of whole

metal and in the second-run cooling curve of clast. The $\gamma \rightarrow \alpha$ transition phenomenon in the first-run cooling curves of bulk, matrix and clast may be masked by magnetization of taenite phase which has a braod range of Curie point of a widely dispresed range in Ni content after the breakdown of tetrataenite phase at elevated temperatures. The kamacite phase of $\theta^*_{\alpha \rightarrow \gamma}$=780~785°C and $\theta^*_{\gamma \rightarrow \alpha}$=665°C correspondes to kamacite of 5.0 wt% Ni.

Fig.3 shows thermomagnetic curves of a man-made 50Fe50Ni alloy, which represents a disordered taenite of 50 wt% Ni, for reference. The thermomagnetic curves are approximately reversible with temperature and Curie point is 515°C. Comparing the thermomagnetic curves of the apprent tetrataenite phase (Fig. 2 (d)) with Fig.3, it will be noted (a) that the heating thermomagnetic curve of St. Séverin apparent tetrataenite phase decreases with temperature much less than that of 50Fe50Ni alloy in a temperature range lower than about 450°C, and (b) that the cooling thermomagnetic curve of St. Séverin apprent tetrataenite is a little less convex than that of 50Fe50Ni alloy, though the general features of the former look similar to those of the latter, and further (c) that the apparent Curie point of the cooling curve is lower than that of the heating curve for St. Séverin apparent tetrataenite phase.

The characteristic feature of thermomagnetic change of tetrataenite that the shape of its first heating thermomagnetic curve is essentially flat up to about 450°C and then drops abruptly to Curie point has already been discussed for Yamato

74160 LL_7 chondrite (Nagata and Fukui, 1982). As for St. Séverin LL_6 chondrite, the first-run heating thermomagnetic curves of apparent tetrataenite component of matrix, clast and whole metal (i.e. magnetization of kamacite component being eliminated) are plotted together with the first-run heating thermomagnetic curve of the extracted apparent tetrataenite specimen itself in Fig.4, where all thermomagnetic curves are normalized at 50°C. It may be concluded in Fig.4 that the thermomagnetic characteristics of tetrataenite phase in matrix and clast of St. Séverin are substantially same as those of extracted relatively large grains (11~53 mg in weight) of whole metal and apparent tetrataenite metal in the first-run heating process.

On the other hand, general features of the first-run cooling thermomagnetic curves of taenite component (i.e. kamacite magnetization being eliminated) in matrix, clast and whole metal are considerably deviated from those of extracted apparent tetrataenite grain and 50Fe50Ni alloy, as shown in Fig.5, where all thermomagnetic curves are normarized at 100°C. Namely, the cooling thermomagnetic curves of taenite components of matrix, clast and whole metal are concave, while those of extracted apparent tetrataenite and 50Fe50Ni alloy are convex. This result may suggest that the original ordered tetrataenite phase is not only broken down to transform to a disordered taenite, but tends to be homogenized with low-Ni taenite phases to form disordered taenites of various Ni-contents of less than 50 wt%.

Fig.6 shows examples of Ni-content spectra of the extracted

apparent tetrataenite sample (top) and the whole metal sample (bottom) after heating to 820°C, obtained by a thermomagnetic analysis of the first-run cooling thermomagnetic curve. Ni-cotent spectra of metallic component in matrix and clast of St. Séverin are approximately simillar to the Ni-content spectrum of the whole metal. Namely, the Ni-content spectra of matrix, clast and whole metal of St. Séverin are spread over a wide range of Ni-content, extending to about 30 wt% Ni on the low-Ni side, in addition to a sharp spectral line of kamacite of 5 wt% Ni.

As already reported (Danon et al., 1979 a), the apparent tetrataenite phase in St. Séverin consists of genuine ordered tetrataenite crystallites (0.15~0.30μm in diameter) and paramagnetic (less than 30 wt% in Ni-content) disorderd taenite matrix according to results of Mössbauer spectral analysis. It seems most likely therefore that tetrataenite crystallites are homogenized with the surrounding low-Ni taenite to form the observed Ni-poorer disordered taenite phases of various Ni-content values at elevated temperatures. In the case of the extracted apparent tetrataenite sample, which is a relatively large grain (11mg in weight) and whose surface is chemically cleaned up, almost no kamacite is detected by an Mössbauer spectral analysis so that the assumed homogenization process of Ni-content might be much less effective at elevated temperatures.

The main interest in the present study is mostly concerned with a possible process of formation of tetrataenite phase from disordered taenites in meteorites in the extraterrestrial space.

It appears in the present study that a process of (Tetrataenite)+(Paramagnetic Taenite)→(Disordered Ferromagnetic Taenite) is possible to take place at elevated temperatures. It seems possible then that a reverse process to form tetrataenite from disordered ferromagentic taenites can take place on appropriate conditions. In the case of St. Séverin, however, the coexistence of kamacite phase also has to be taken into account.

2.4 Natural remanent magnetization

The natural remanent magnetization (NRM) of St. Séverin bulk sample is extremely stable against the AF-demagnetization, as shown by examples given in Fig.7 (a) and (b), where the intensity and direction of residual NRM after AF-demagnetizing up to $\tilde{H}$ (in Oe peak) are plotted. The residual NRM intensity after AF-demagnetizing up to 1800 Oe peak still keeps about 70% of the initial value, though some intensity fluctuations due to an inhomogeneity of NRM are involved in the AF-demagnetization curve. The residual NRM direction during the course of AF-demagnetization is one-directionally changed by about 40° in angle, but it is settled within 10° in angle around the mean direction for $\tilde{H}$ values larger than 300~400 Oe peak, suggesting that St. Séverin meteorite possesses an extremely stable major component of NRM.

Figures 8 and 9, show thermal demagnetization behaviours in

intensity and direction respectively for the stable NRM component of St. Séverin bulk specimen after AF-demagnetizing up to 1200 Oe peak. In Fig.8, the thermal demagnetization curves of NRM for two specimens, (b) and (c), are not simply monotonous but associated with some fluctuations, suggesting that NRM of St. Séverin meteorite consists of some heterogeneous components, probably caused by a variety of ordering degree of tetrataenite structure. Generally speaking, however, the extremely stable NRM component possessed by the tetrataenite component is thermally demagnetized almost completely between 500°C and 560°C in temperature, a small portion of NRM still remaining at temperatures above 560°C. Fig.9 shows that the direction of NRM is kept approximately invariant for temperatures below 450~500°C during the course of thermal demagnetization, suggesting that the direction of NRM posessed by the tetrataenite component is reasonably stable within the temperature range. In the heating process above 500°C, the NRM direction changes largely up to almost 600°C, and then it is again stably settled at temperatures higher than 600°C, suggesting that a remaining NRM of a much smaller magnitude is possessed by the kamacite component at the elevated temperatures.

It may be generally concluded that NRM of St. Séverin meteorite is extremely stable as far as temperature is lower than about 400°C and the main parts of the stable NRM are possessed by the tetrataenite component. However, the acquisition process for the unusually stable NRM of tetrataenite phase has not yet been

definitely identified.

3 APPLEY BRIDGE (LL_6) and TUXTUAC (LL_5) CHONDRITES

Both Appley Bridge and Tuxtuac are "fell" meteorities; Appley Bridge fell on England on October 13, 1914, and Tuxtuac fell on Mexico on October 16, 1975. Wasilewski (1982) has already experimentally demonstrated that Appley Bridge LL_6 chondrite also shows the characteristic features of thermomagnetic curves of tetrataenite phase. In the present work, composition and structure of metallic components of Appley Bridge and Tuxtuac chondrites are first determined, and then magnetic properties of their bulk specimens are examined.

3.1. Composition and structure of metal

The average composition of Appley Bridge metal, determined with the aid of Mössbauer spectral analysis, is approximately given by

(Tetrataenite):(Disordered taenite):(Kamacite)=80:20:($\sim$0)

(in wt%).

The average composition of metals in Tuxtuac determined by the same Mössbauer spectral analysis is approximately given by

(Tetrataenite):(Disordered taenite):(Kamacite)=15:85:($\sim$0)

(in wt%).

In both chondrite metals, kamacite phase is hardly detectable in the Mössbauer spectral analysis, and the share ratios of ordered tetrataenite to disordered taenite in the two LL chondrites are approximately reversed to each other.

3.2. Basic magnetic properties

Basic magnetic hysteresis curve parameters measured at room temperature and at liquid He temperature of bulk specimens of Appley Bridge and Tuxtuac LL chondrites before and after heating to 820°C are summarized in Table 3. Just as in the case of St. Séverin, Hc and I_R/I_S values of Appley Bridge are drastically reduced by the heat treatment, indicating a breakdown of the ordered tetrataenite structure to the disordered taenite by the heat treatment. The decreasing changes of H_C and I_R/I_S values of Tuxtuac caused by the heat treatment are considerably smaller than those of Appley Bridge, indicating that the share ratio of tetrataenite phase in Tuxtuac metal is much smaller than that in Appley Bridge metal.

3.3. Thermomagnetic curve characteristics

Figures 10 and 11 show the first-run and second-run thermomagnetic curves of Appley Bridge and Tuxtuac respectively. As Curie point is 565°C and no kamacite phase is detected in Appley Bridge thermomagnetic curves, its ferromagnetic metallic

component may consist of tetrataenite and disordred taenite of about 50% Ni in the original state. Actually, the first-run heating thermomagnetic curve has the characteristic flatness of tetrataenite for a temperature range up 450°C, and the cooling thermomagnetic curves after the breakdown of tetrataenite phase by the heat treatment are approximately identical, in shape, to the cooling thermomagnetic curve of 50Fe50Ni alloy shown in Fig.3.

In the Tuxtuac thermomagnetic curves, the characteristic flatness of the first-run heating thermomagnetic curve for tetrataenite phase appears to be superimposed on an ordinary thermomagnetic curve of disordred taenite phase, because relative content of tetrataenite phase is only 3/17 of disordered taenite phase.

Although a small amount of kamacite phase of $\Theta^*_{\alpha\to\gamma}$=780°C can be detected in the first-run heating thermomagnetic curve of Tuxtuac, it seems very likely that the kamacite phase is much reduced to a too small amount to be magnetically detected in the second-run heating curve. The first-run cooling thermomagnetic curve and the second-run curves of Tuxtuac are concave in a temperature range from 600°C to 300°C and are essentially different from the convex cooling thermomagnetic curve of Appley Bridge as well as 50Fe50Ni alloy. With the aid of the same analysis method for St. Séverin, the Ni-content spectra of metallic component after the heat treatment for Appley Bridge and Tuxtuac are obtained as shown in Fig.12. As indicated in Fig.10,

the main components of metals after the heat treatment in Appley Bridge are disordered taenites of 50-60 wt% Ni, though a small amount of Ni-poor taenite of about 30 wt% Ni still coexists. As indicated in Fig.11, on the other hand, the metallic components in Tuxtuac after the heat treatment are represented by a broad continuous band of Ni-contnet in taenite extending from 30 wt% Ni to 60 wt% Ni and having a maximum peak around 40 wt% Ni. No spectral line of kamacite phase is detectable in the Ni-content spectrum of Tuxtuac after the heat treatment, though about 7 wt% of kamacite phase of 5 wt% Ni in metal is magnetically detected in the first-run heating thermomagnetic curve. only a possible interpretation of the observed disappearance of kamacite phase by heating will be a homogenization of kamacite phase with neighbouring taenite phases.

4 THERMOMAGNETIC CHARACTERISTICS OF TETRATAENITE-RICH

Meteorites

Thermomagnetic behaviours of tetrataenite phase can be characterized by several measurable factors. One of the characteristic factors will be a sharp irreversible magnetic transition in the first-run heating thermomagnetic curve, examples of which are typically represented by Fig 2.(d) for an extracted piece of apparent tetrataenite of St. Séverin and by Fig.10 for Appley Bridge chondrite. The magnetic transition

temperature, which is considered as Curie point of tetrataenite phase, is ranged between 560°C and 570°C as summarized in Table 4, where observed values of $\Theta^*_{\alpha\rightarrow\gamma}$ and $\Theta^*_{\gamma\rightarrow\alpha}$ of coexisting kamacite phase, if any, also are given. In the cases of Yamato 74160 and Appley Bridge, their second-run thermomagnetic curves clearly show a single Curie point of the transformed disordered taenite of about 55 wt% Ni around 550°C, so that it will be highly plausible that their sharp magnetic transition point at 560-565°C in the first-run heating thermomagnetic curve corresponds to Curie point (H_C) of tetrataenite phase. Since, however, Curie points of Fe-Ni alloy at 560° and 570° correspond respectively to 57 wt% and 59 wt% in Ni content on the basis of a Curie point versus Ni-content relationship for taenite given by Crangle and Hallam (1963) and an expected Curie point of a stoichiometric tetrataenite composition (i.e. 48.8 wt% Fe, 51.2 wt% Ni) will be about 505°C, there will be a possibility that Curie point of the ordered tetrataenite is a little higher than Curie point of discrdered taenite of the same chemical composition.

In order to ascertain the sharp irreversible magnetic transition phenomenon of tetrataenite-rich metal, magnetic characteristics of Santa Catharina Ni-rich ataxite, which has been crystallographically studied in detail to prove that the ordered tetrataenite is its main constituent (Danon et al., 1979 b),are examined as much precisely as possible. The chemical composition of tetrataenite phase in Santa Catharina is (48-49) wt%Fe (50-51) wt%Ni, while the characteristic sharp magnetic

transition point temperature (Θ_C) is 565°C, as shown in Fig.13. Taking into consideration thermomagnetic characteristics of an extracted piece of apparent tetrataenite phase of St. Severin shown in Fig.2(d) also, it may be concluded that the ordered tetrataenite has a sharp magnetic transition point at 560-565°C, and it may be Curie point of the ordered tetrataenite structure.

A similar sharp magnetic transition at 560-570°C observed in the other meteorites, in which kamacite phase coexists, can be interpreted in the same way.

The second point may be concerned with characteristics of the cooling thermomagnetic curve after the breakdown of the ordered tetrataenite structure by heating. In the cases of Yamato 74160 and Appley Bridge, their cooling thermomagnetic curves may represent mostly the reversible thermomagnetic curve of disordered taenite of 50-55 wt% in Ni-content. However, the original values of magnetic coercive force (H_C) at room temperature of Yamato 74160 and Appley Bridge are only 255 Oe (Nagata and Funaki, 1982) and 160 Oe (Table 3) respectively, which are much smaller than the expected H_C value of tetrataenite itself. In fact, the observed H_C value of Santa Catharina Ni-rich ataxite at room temperature amounts to 2,800 Oe. Since the magnetic coercive force (H_O) of a tetrataenite crystal along its uniaxial easy axis is H_O=4,900 Oe, the observed H_C value of Santa Catharina is reasonable for an assemblage of almost randomly oriented tetrataenite microcrystallites.

As already discussed (Nagata and Funaki, 1982), the magnetic

coercive force of a mixture of a magnetically hard component having a large coercive force and a soft component having a small coercive force is affected more largely by the soft component than by the hard component, thus resulting in a much smaller resultant coercive force than the coercive force of the hard component. Assuming then that the magnetic coercive force of an assemblage of randomly oriented tetrataenite microcrystallites is 2,800 Oe, weight content (m) of tetrataenite phase in metallic components of Yamato 74160 and Appley Bridge are estimated as m=43 wt% for Yamato 74160 and m=67 wt% for Appley Bridge, where the soft components are disordered taenite of H_C=8 Oe for Yamato 74160 and disordered taenite of H_C=4.5 Oe for Appley Bridge. It is observed by an electron microprobe analysis that the chemical composition of disordered taenite phase is about 50 wt% Ni in Yamato 74160. Therefore, the first-run cooling curve after the breakdown of tetrataenite structure shows a typical convex curve which is very similar to the thermomagnetic curves of 50Fe50Ni alloy (Fig.3), and the Ni-content spectra corresponding to these thermomagnetic curves consist of spectral lines concentrated around 50% Ni. Thermomagnetic curve characteristics and the corresponding Ni-content spectra for Appley Bridge are very similar to those of Yamato 74160, so that the disordered taenite phase of Appley Bridge also will be around 50% Ni in chemical composition. Thermomagnetic characteristics of the apparent tetrataenite piece extracted from St. Severin metal also show similar characteristics, probably because the chemical

composition of remaining disordered taenite is near 50% Ni in composition, as suggested by Fig.6.

On the other hand, Ni-content spectra of taenite component in the whole metal of St. Séverin (Fig.6, bottom) and in Tuxtuac (Fig.12, bottom) are spread over a fairly wide range of Ni-content (30-60 wt%) after the breakdown of tetrataenite phase by heating. As already discussed individually for the cases of St. Séverin and Tuxtuac, it seems very likely that fine ordered tetrataenite specks of 50Fe50Ni in atomic composition are not simply broken down to the disordered taenite structure but also tend to be homogenized with surrounding low-Ni taenites, and probably even with kamacite, at elevated temperatures. This hypothesis of homogenization of Ni content in the disordered taenite (namely, f.c.c. structure of Fe-Ni alloy) after the breakdown of tetrataenite structure at elevated temperatures may need further experimental certifications with respect to microstructure of the metallic grains concerned before and after the heat treatment. It seems, however, that an example of thermomagnetic characteristics of Santa Catharina Ni-rich ataxite, shown in Fig.13, may support the hypothesis of homogenization of Ni content. In Fig.13, the first-run heating and cooling thermomagnetic curves and the second-run cooling thermomagnetic curve of Santa Catharina are shown. The second-run heating thermomagnetic curve is almost identical to the first-run cooling curve, and the third-run heating and cooling thermomagnetic curves are almost same as the second-run

cooling curve. Namely, the first-run cooling and second-run heating thermomagnetic curves after the first heat treatment show that the ferromagnetic metal consists of two main components, a component having Curie point at 500°C-550°C (corresponding to 50-55 wt% Ni) and the other component having Curie point at 250~300°C (corresponding to 35~40 wt% Ni), while the second-run cooling and the third-run heating and cooling thermomagnetic curves after the second and third heat treatments show that the ferromagnetic metal consists of a continuous spectra of Ni content in a range of 30-55 wt% Ni, as in the cases of St. Séverin whole metal and Tuxtuac.

5 CONCLUDING REMARKS

In the present study, magnetic properties of Appley Bridge, Tuxtuac and St. Séverin tetrataenite-rich chondrites are examined in comparison with Yamato 74160 tetrataenite-rich chondrite, Santa Catharina Ni-rich ataxite and an artificially made 50Fe50Ni alloy. In particular, bulk specimens, matrix, clast, metallic grains and an extracted piece of apparent tetrataenite phase of St. Séverin are separately examined in some detail.

Ferromagnetic features of tetrataenite component in meteorites are characterized by (a) a high magnetic coercivity represented by unusually large values of H_C and H_{RC}, (b) an

essential flatness of thermomagnetic curve in a temperature range below about 450°C, as shown in Fig.4, and (c) a breakdown of these typical magnetic characters of tetrataenite structure by heating up to temperature above Curie point during a relatively short pericd, i.e, an hour in order of magnitude. Because of the high magnetic coercivity of tetrataenite component, NRM of tetrataenite-rich meteorite contains an extremely stable component which is hardly AF-demagnetized even by 2,000 Oe in alternating magnetic field intensity, as demonstrated for Yamato 74160, Allan Hills 77260 and St. Séverin chondrites.

However, the formation process for the tetrataenite phase in meteorites and the acquisition mechanism for the stable NRM of tetrataenite-rich meteorites have not yet been definitely clarified. As each orderd tetrataenite phase in meteoritic metals occupies only a very fine volume of several um or less in mean diameter in matrix of disorderd taenite, microscopic examinations, both crystallographically and magnetically, of tetrataenite phases in meteoritic metals in much more detail will be required in further studies.

FIGURE CAPTIONS

Fig 1. First-run and second-run thermomagnetic curves of bulk specimen of St. Severin LL_6 chondrite.

Fig 2. First-run and second-run thermomagnetic curves of (a) matrix, (b) clast, (c) whole metal and (d) extracted apparent tetrataenite piece of St. Severin.

Fig 3. Thermomagnetic curve of man-made 50Fe50Ni alloy.

Fig 4. Heating thermomagnetic curves of tetrataenite components in matrix, clast and whole metal in comparison with apparent tetrataenite.

Fig 5. Cooling themomagnetic curves of tetrataenite components after breakdown of tetrataenite structure by heating in comparison with thermomagnetic curve of 50Fe50Ni alloy of disordered taenite structure.

Fig 6. Ni-content spectra for extracted tetrataenite piece (top) and whole metal piece (bottom) of St. Severin.

Fig 7. AF-demagnetization curves of NRM of 2 bulk specimens of St. Severin. (Top) Intensity change. (Bottom) Direction change.

Fig 8. Thermal demagnetization curves of NRM intensity of 2 bulk specimens of St. Severin.

Fig 9. Changes in direction during thermal demagnetization of NRM of 2 bulk specimens of St. Severin.
Specimen (b), (top) and Specimen (c), (bottom).

Fig 10. First-run and second-run thermomagnetic curves of Appley Bridge LL_6 chondrite.

Fig 11. First-run and second-run thermomagnetic curves of Tuxtuac LL_5 chondrite.

Fig 12. Ni-content spectra in metallic component for Appley Bridge (Top) and Tuxtuac (Bottom).

Fig 13. First-run thermomagnetic curves and second-run cooling thremomagnetic curve of Santa Catharina Ni-rich ataxite.

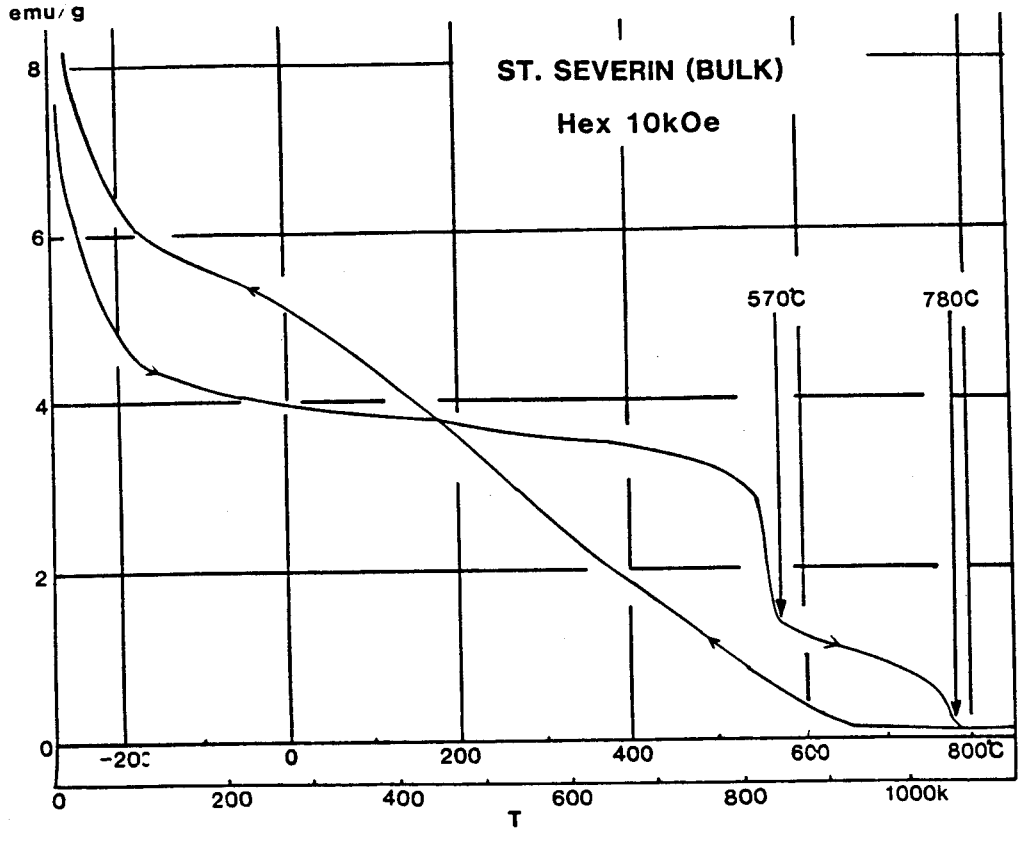
emu/g
8
6
4
2
0
ST. SEVERIN (BULK)
Hex 10kOe
570C
780C
-20C
0
200
400
600
800C
0
200
400
600
800
1000k
T

Fig. 1

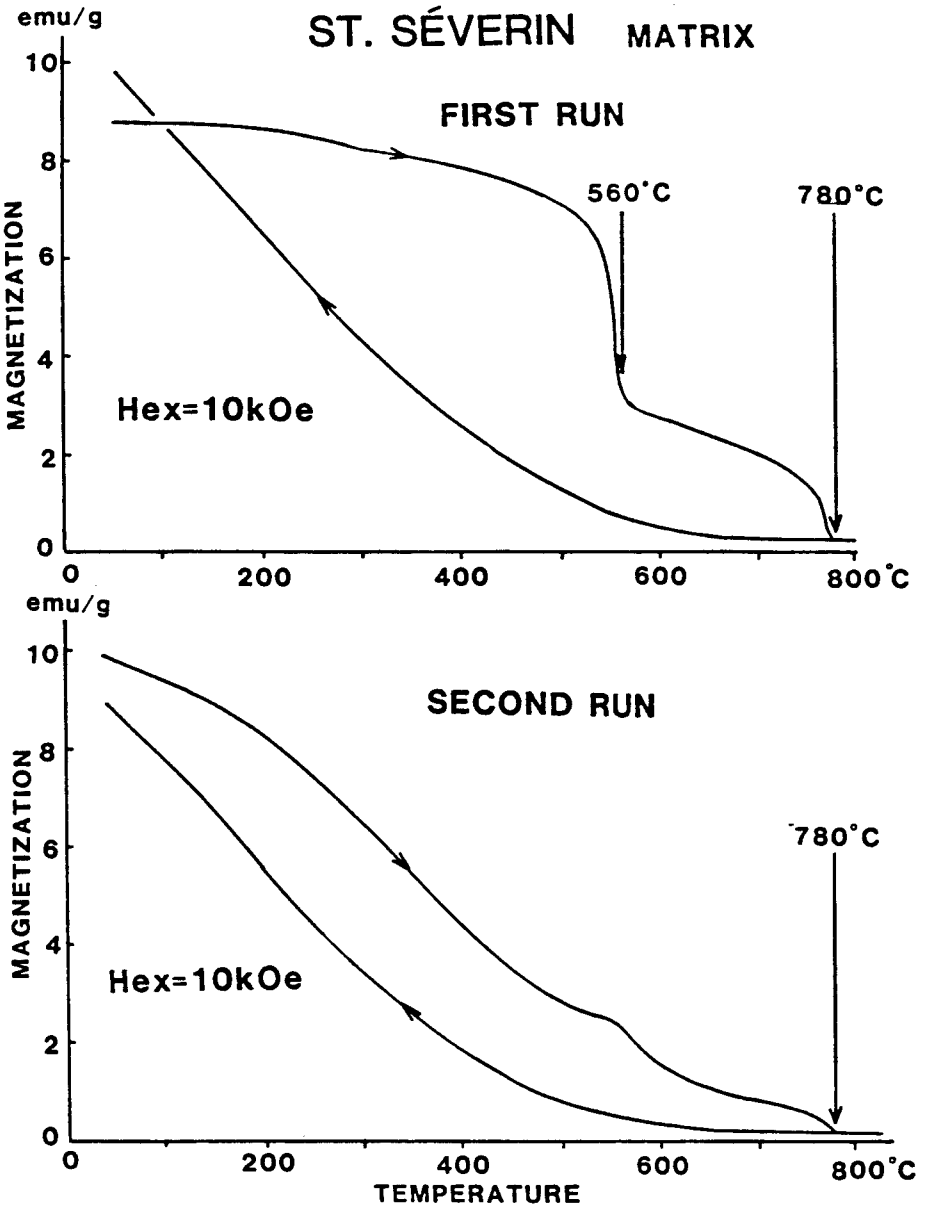
ST. SÉVERIN MATRIX
FIRST RUN
emu/g
MAGNETIZATION
Hex=10kOe
560°C
780°C
SECOND RUN
TEMPERATURE
0
200
400
600
800°C
2
4
6
8
10

Fig. 2(a)

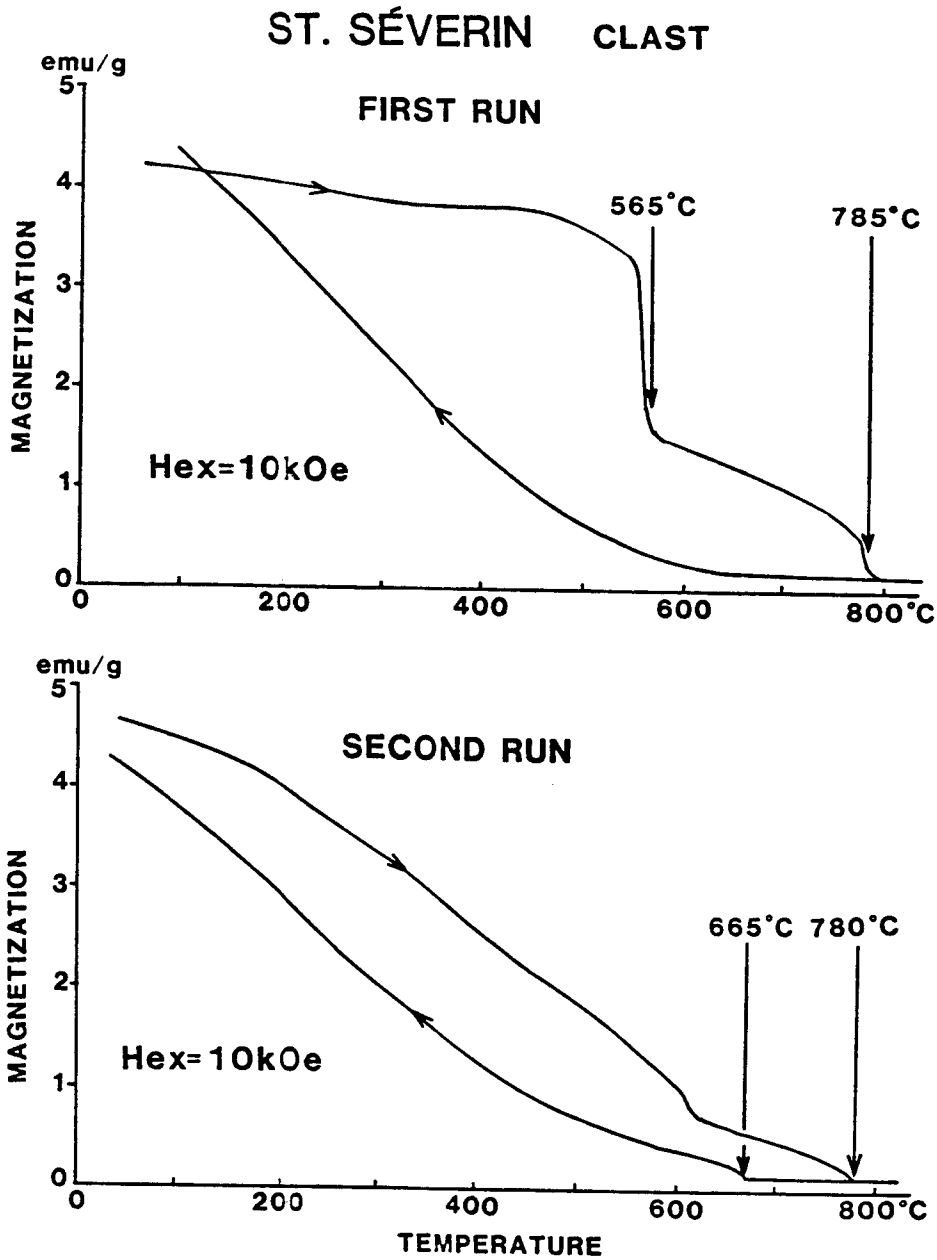
ST. SÉVERIN CLAST
emu/g
FIRST RUN
MAGNETIZATION
565°C
785°C
Hex=10kOe
0
200
400
600
800°C
emu/g
SECOND RUN
MAGNETIZATION
665°C
780°C
Hex=10kOe
TEMPERATURE

Fig. 2(b)

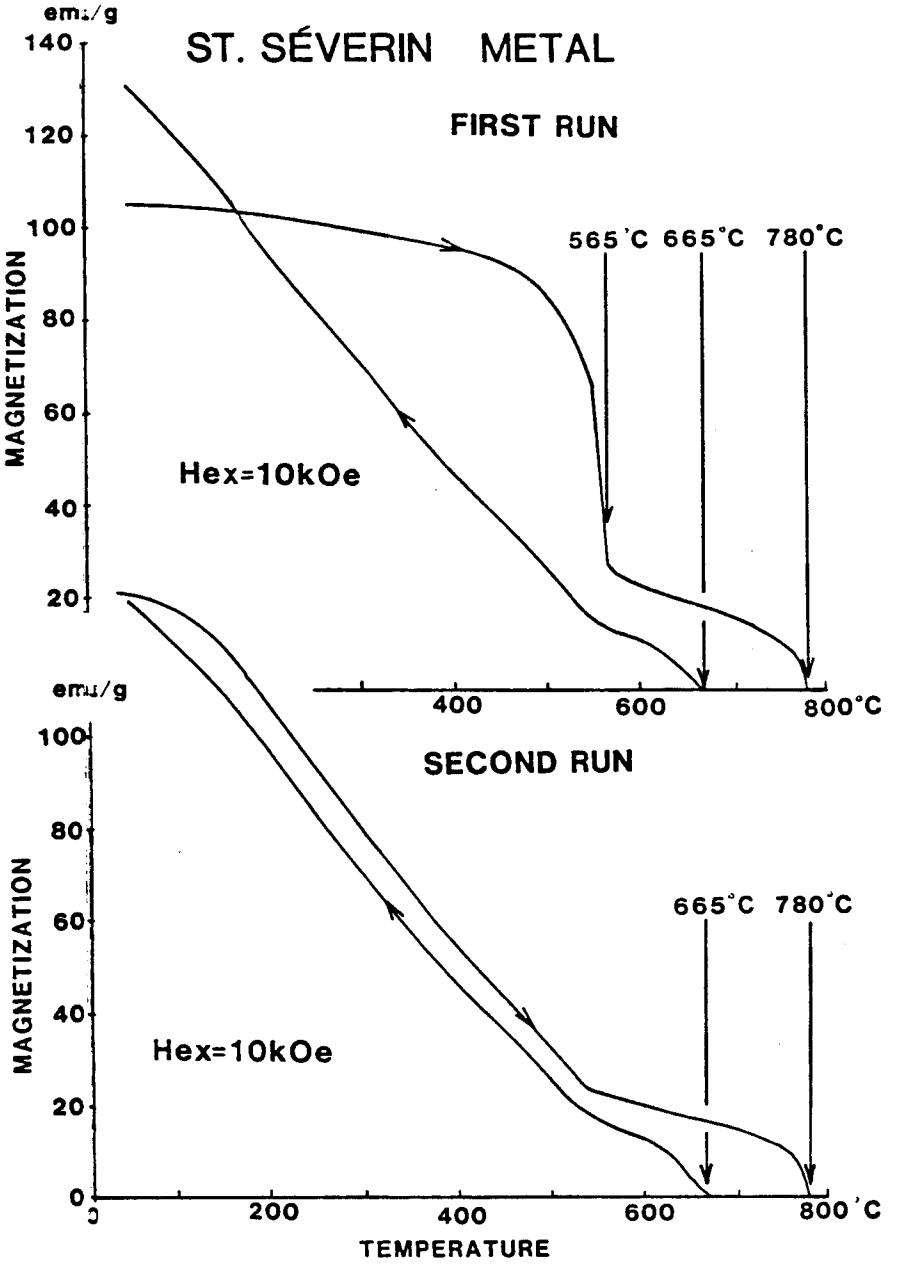
emu/g
ST. SÉVERIN METAL
FIRST RUN
565°C 665°C 780°C
MAGNETIZATION
Hex=10kOe
140
120
100
80
60
40
20
400
600
800°C
emu/g
SECOND RUN
665°C 780°C
MAGNETIZATION
Hex=10kOe
100
80
60
40
20
0
200
400
600
800°C
TEMPERATURE

Fig. 2(c)

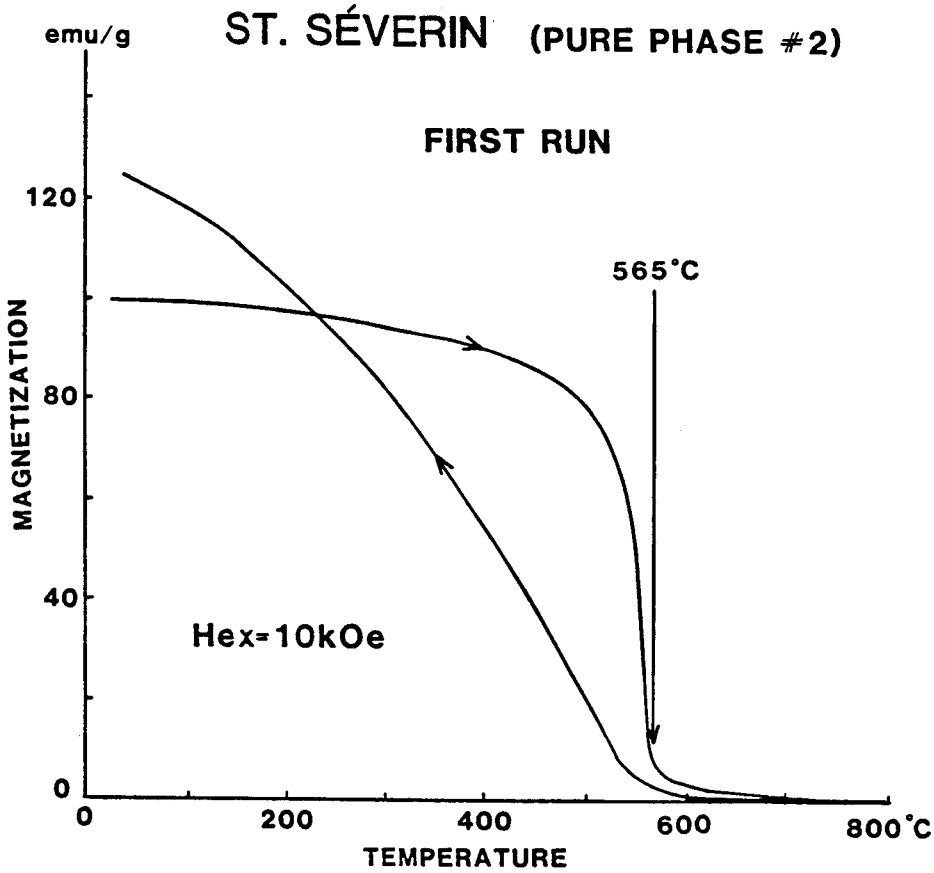
emu/g
ST. SÉVERIN (PURE PHASE #2)
FIRST RUN
120
80
40
0
565°C
MAGNETIZATION
Hex=10kOe
0
200
400
600
800°C
TEMPERATURE

Fig. 2(d)

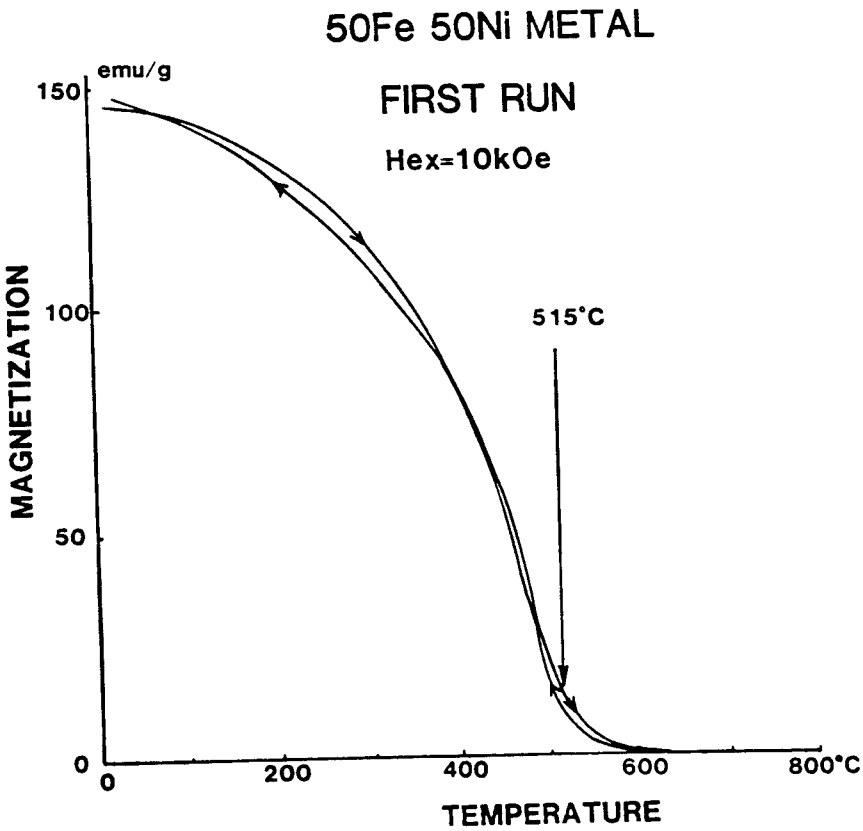
50Fe 50Ni METAL
FIRST RUN
Hex=10kOe
emu/g
150
100
50
0
MAGNETIZATION
515°C
0
200
400
600
800°C
TEMPERATURE

Fig. 3

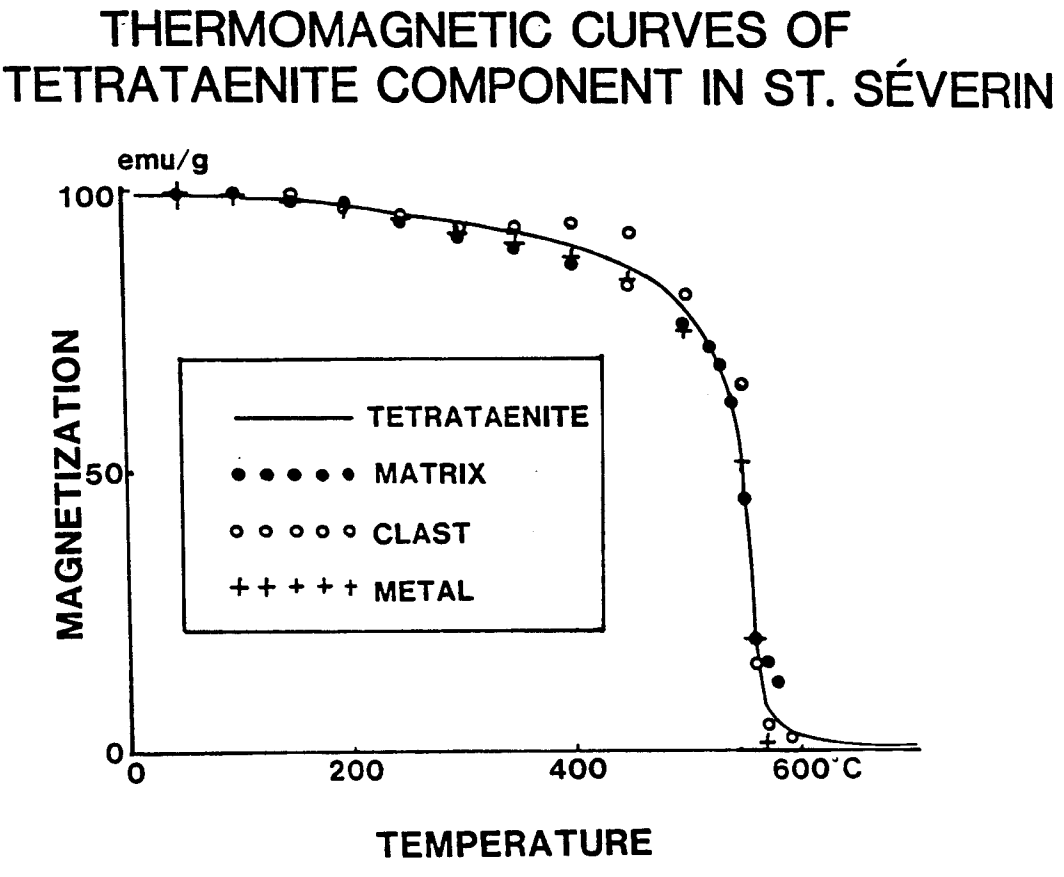
THERMOMAGNETIC CURVES OF
TETRATAENITE COMPONENT IN ST. SÉVERIN
emu/g
100
50
0
MAGNETIZATION
TETRATAENITE
MATRIX
CLAST
METAL
0
200
400
600°C
TEMPERATURE

Fig. 4

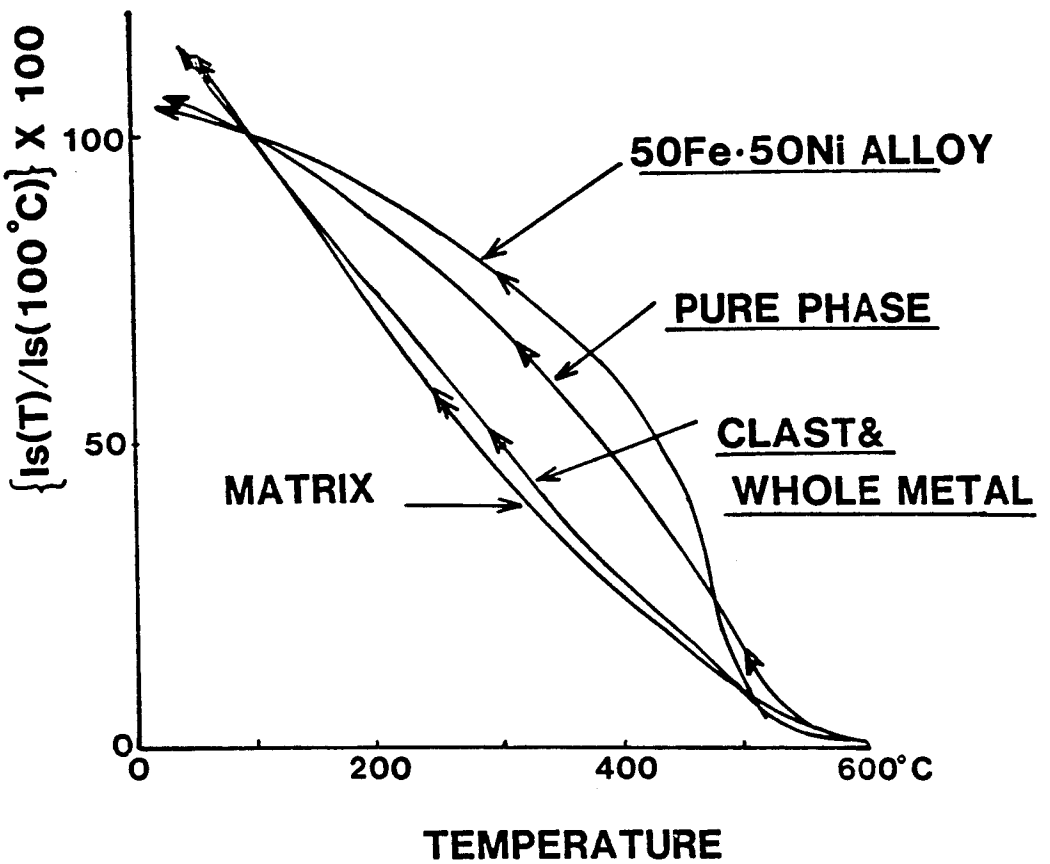
{Is(T)/Is(100°C)} X 100
100
50
0
0
200
400
600°C
TEMPERATURE
50Fe·50Ni ALLOY
PURE PHASE
CLAST&
WHOLE METAL
MATRIX

Fig. 5

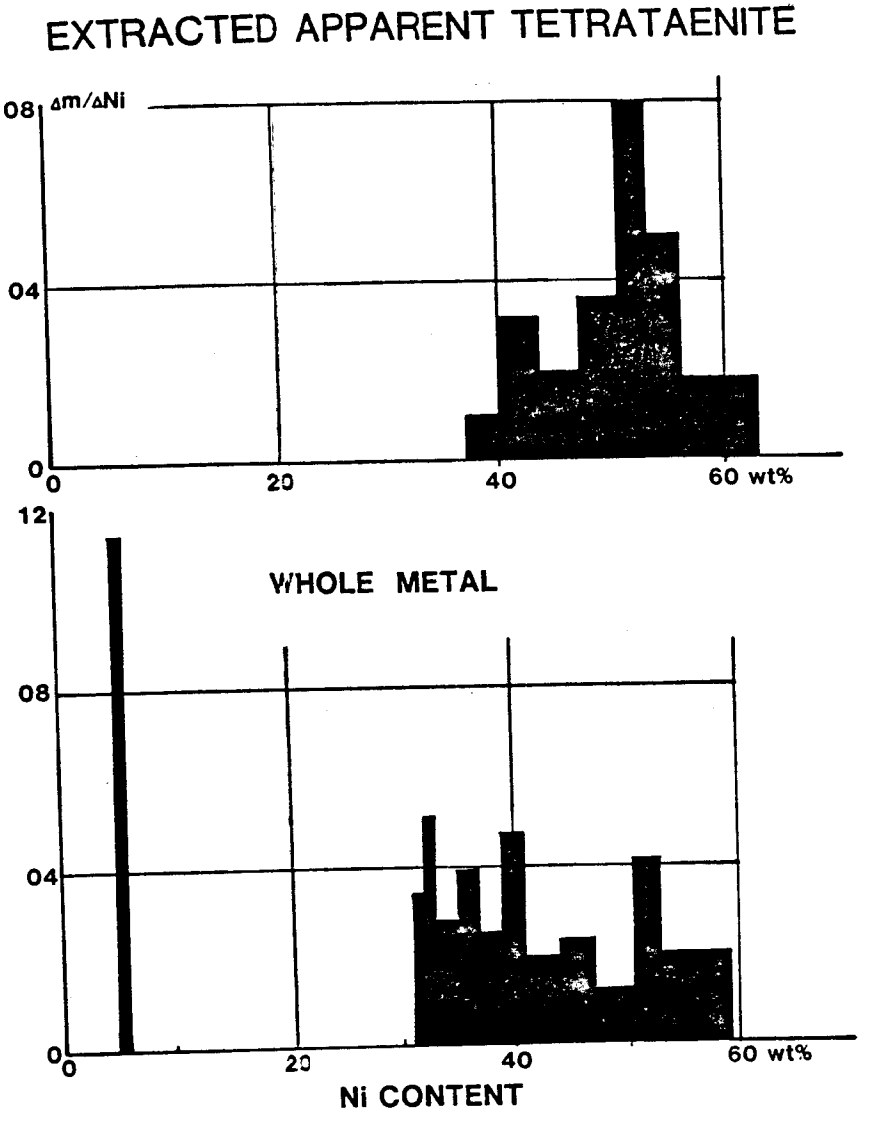
EXTRACTED APPARENT TETRATAENITE
08
Δm/ΔNi
04
0
0
20
40
60 wt%
12
WHOLE METAL
08
04
0
0
20
40
60 wt%
Ni CONTENT

Fig. 6

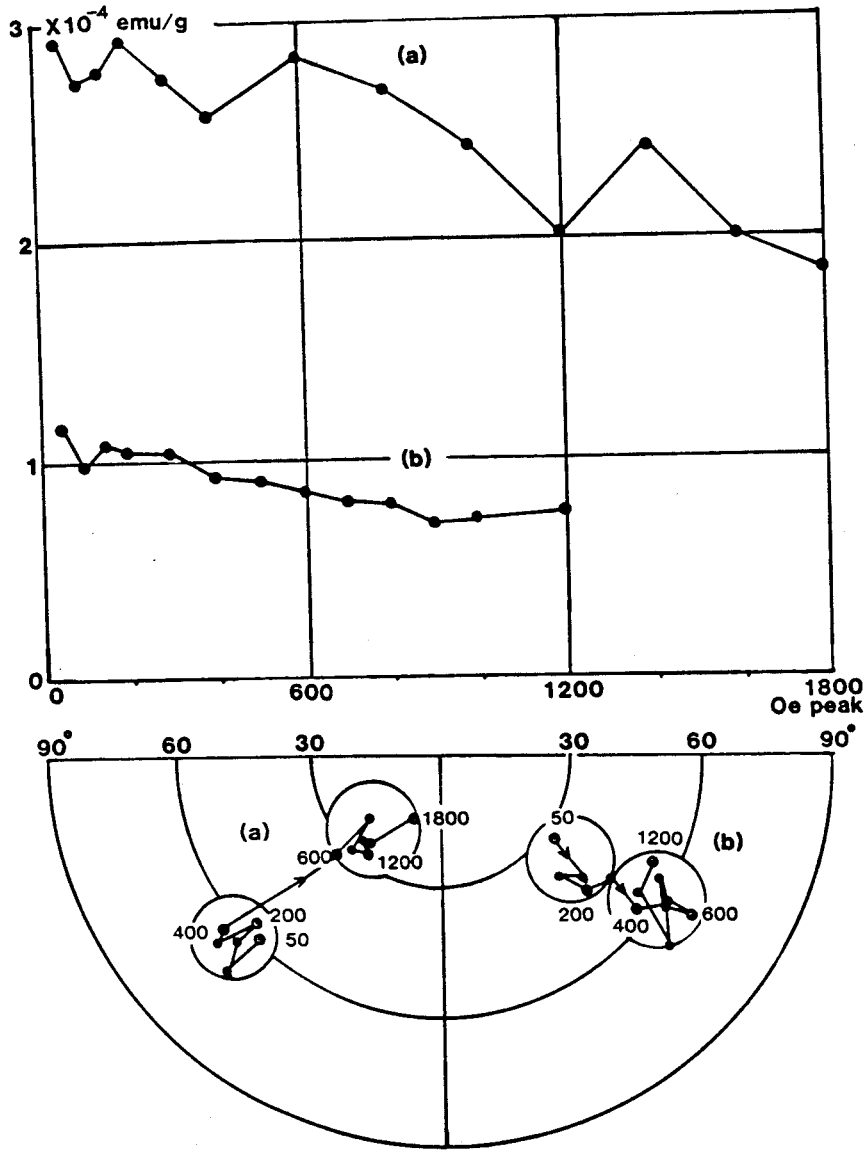
3
X10⁻⁴ emu/g
(a)
2
(b)
1
0
0
600
1200
1800
Oe peak
90°
60
30
30
60
90°
(a)
1800
600
1200
400
200
50
50
1200
(b)
200
400
600

Fig. 7

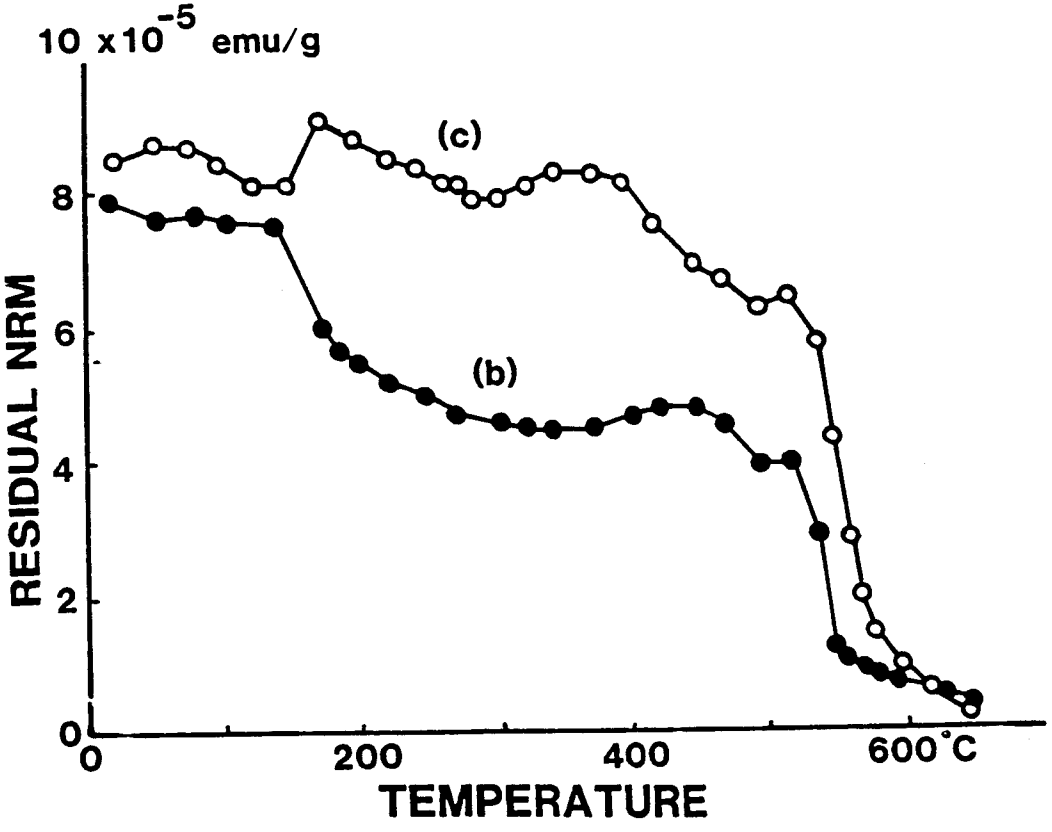
10 x10^-5 emu/g
RESIDUAL NRM
(c)
(b)
8
6
4
2
0
0
200
400
600°C
TEMPERATURE

Fig. 8

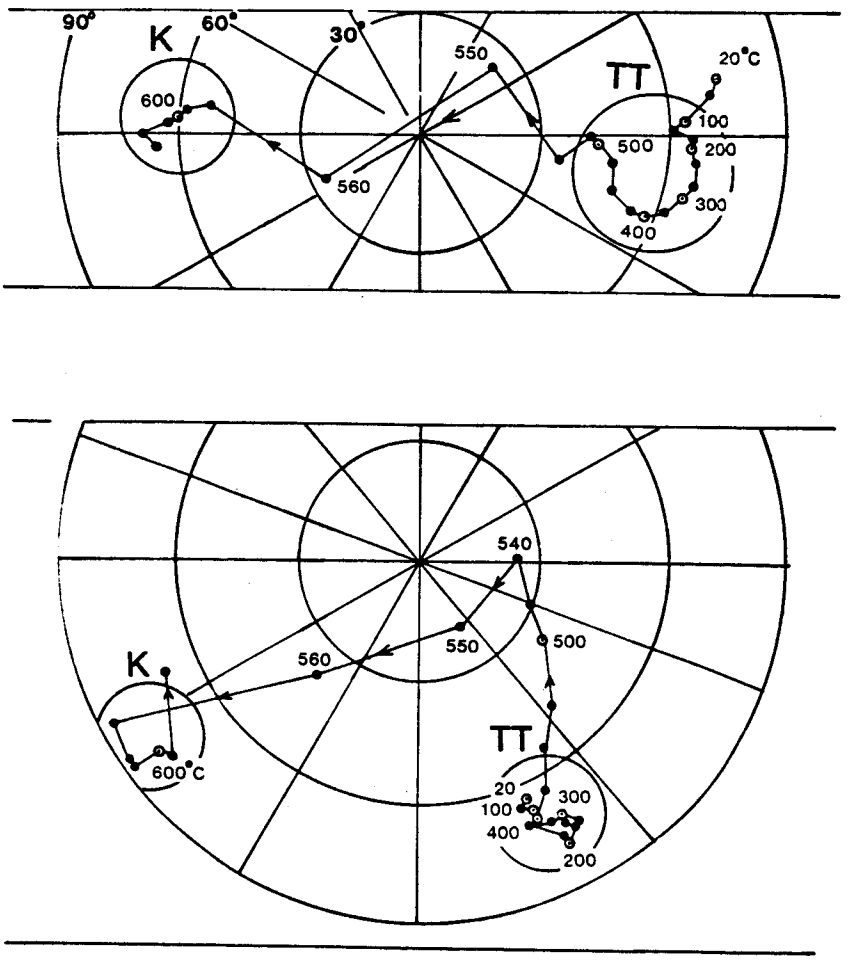
90°
K
60°
30°
550
TT
20°C
600
100
500
200
560
300
400
540
550
500
560
K
600°C
TT
20
300
100
400
200

Fig. 9

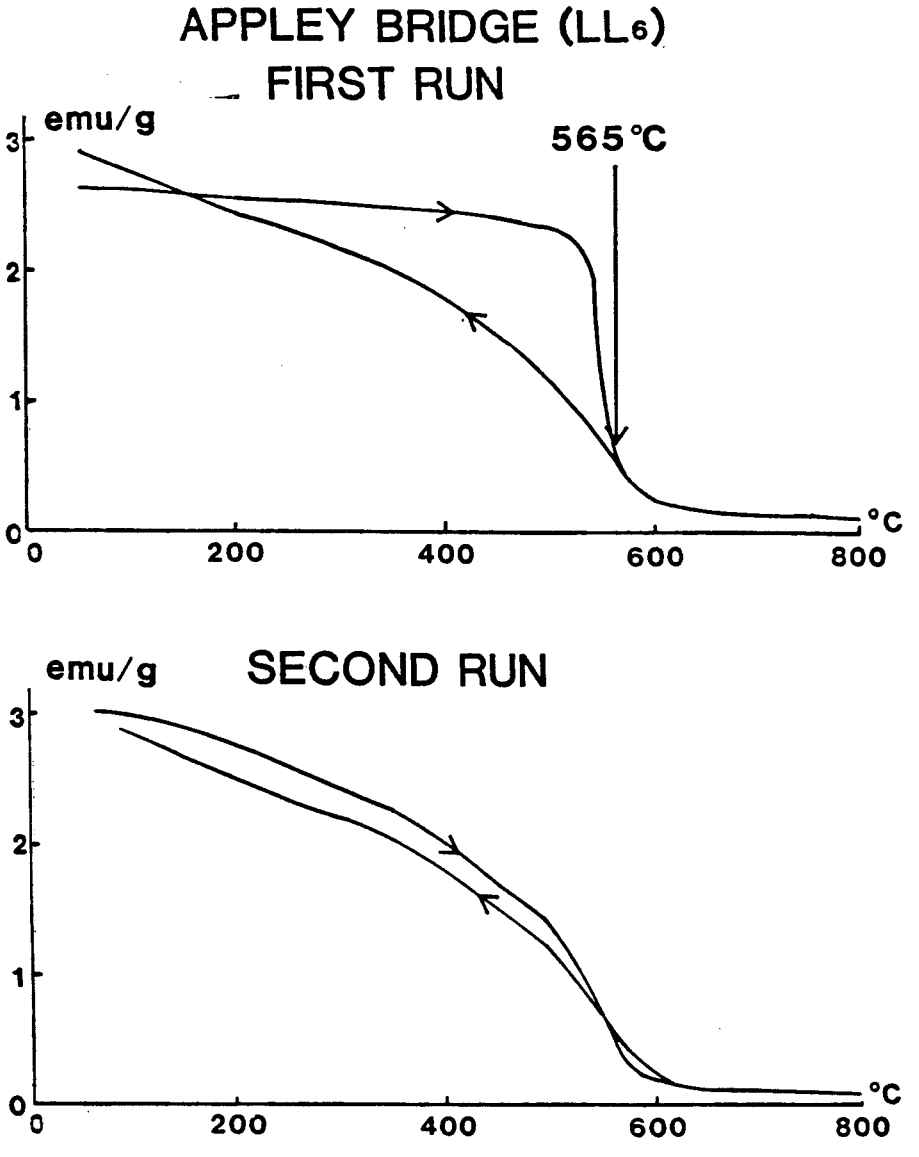
APPLEY BRIDGE (LL6)
FIRST RUN
emu/g
565°C
3
2
1
0
0
200
400
600
800
°C
emu/g
SECOND RUN
3
2
1
0
0
200
400
600
800
°C

Fig. 10

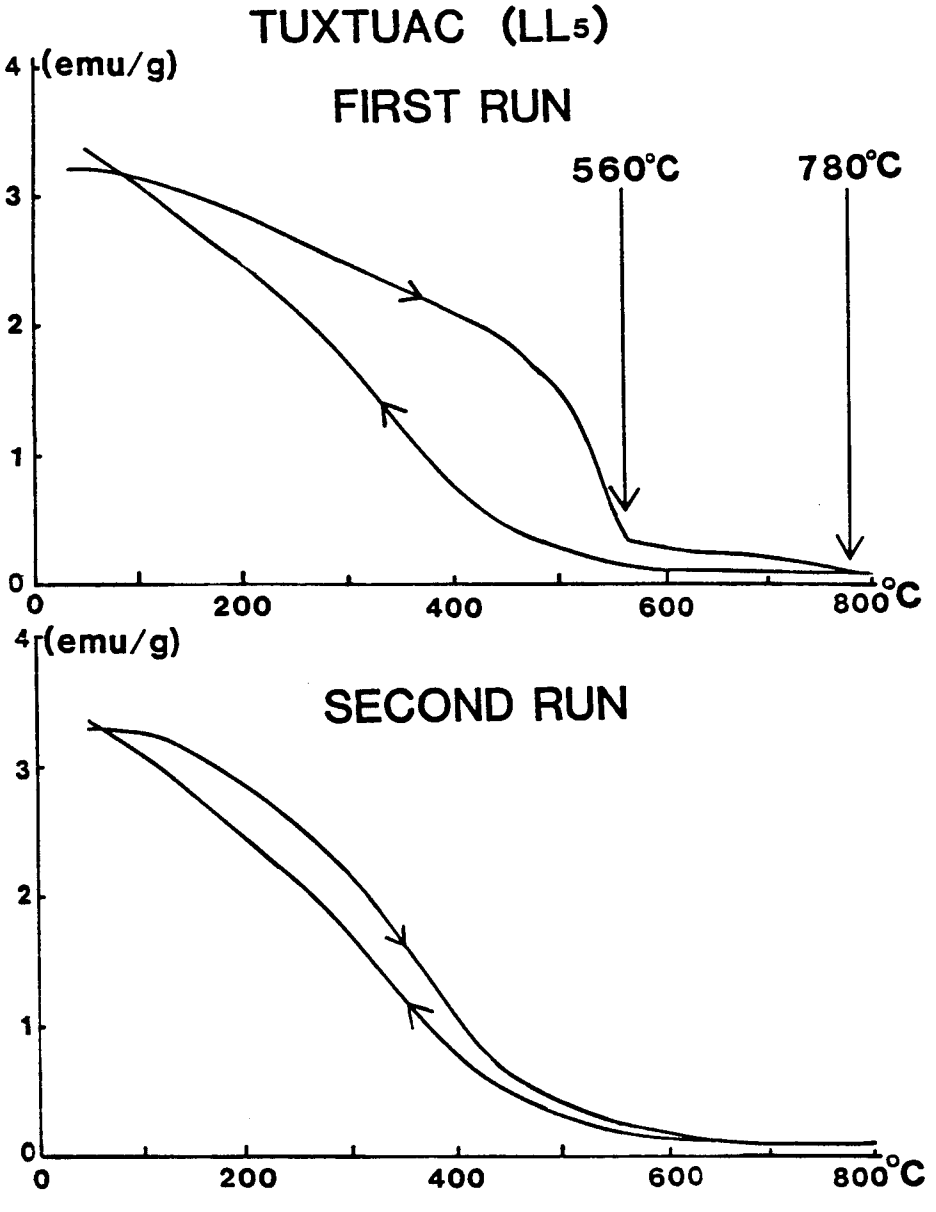
TUXTUAC (LL5)
FIRST RUN
4 (emu/g)
3
2
1
0
560°C
780°C
0
200
400
600
800°C
4 (emu/g)
SECOND RUN
3
2
1
0
0
200
400
600
800°C

Fig. 11

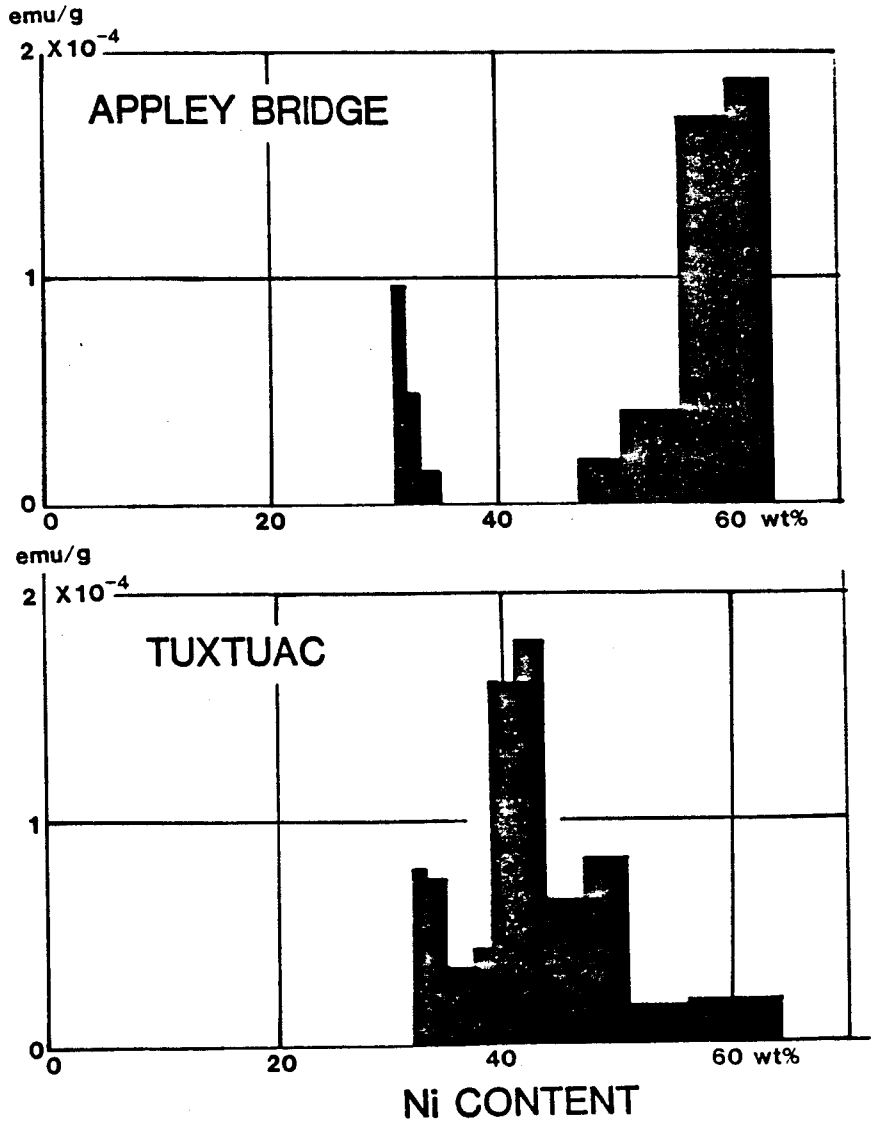
emu/g
2 X10^{-4}
APPLEY BRIDGE
1
0
0
20
40
60 wt%
emu/g
2 X10^{-4}
TUXTUAC
1
0
0
20
40
60 wt%
Ni CONTENT

Fig. 12

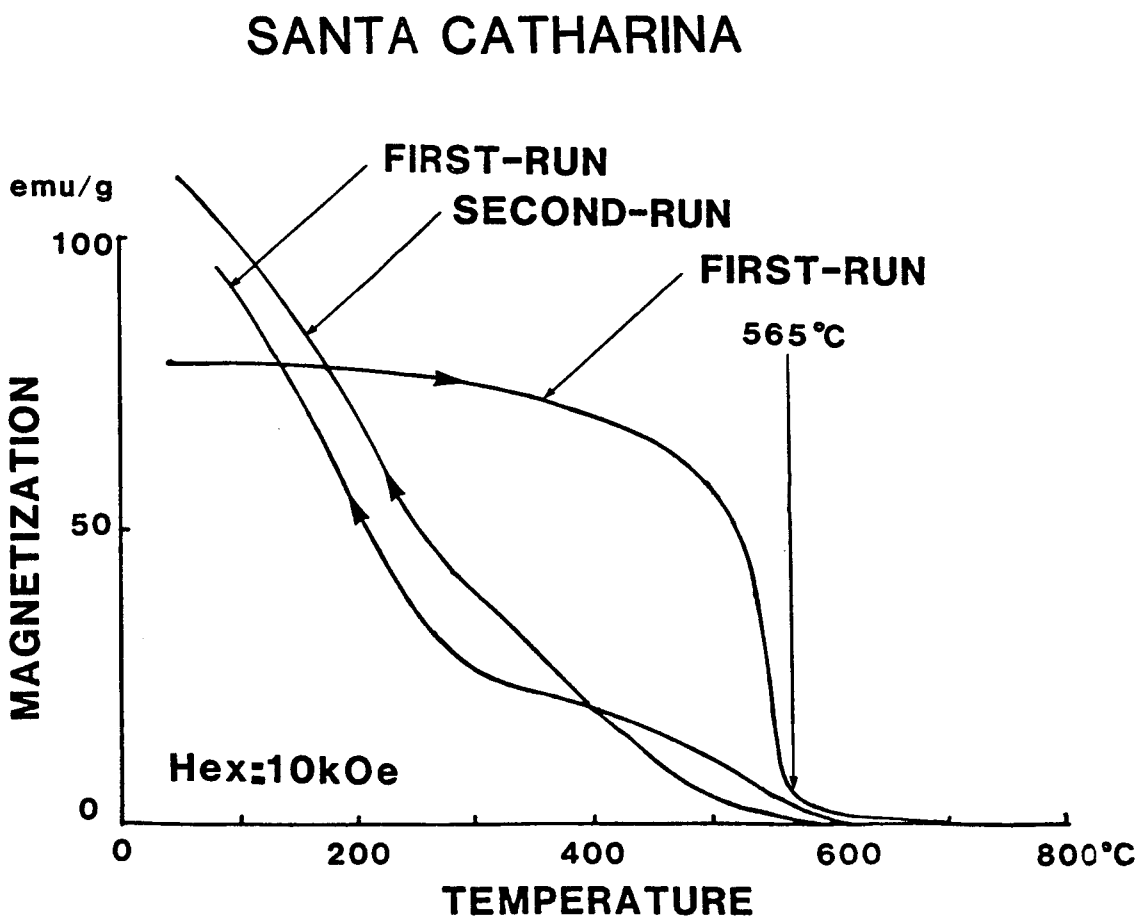
SANTA CATHARINA
FIRST-RUN
SECOND-RUN
FIRST-RUN
565°C
emu/g
100
50
0
MAGNETIZATION
Hex:10kOe
0
200
400
600
800°C
TEMPERATURE

Fig. 13

Table 1. Chemical Composition of Opaque Minerals in St. Séverin

phase	Fe	Ni	Co	S	Total
		(Wt%)			
(taenite)	59.24	41.30	0.79	0.00	101.33
〃	57.37	43.24	0.61	0.00	101.21
〃	53.33	45.09	0.29	0.00	98.71
〃	52.56	45.45	0.51	0.03	98.55
〃	58.25	40.29	1.38	0.00	99.92
〃	54.80	44.95	1.08	0.00	100.83
(Kamacite)	93.36	5.25	2.80	0.01	101.42
〃	91.85	5.13	4.20	0.01	101.19
〃	91.23	5.15	3.54	0.04	99.96
〃	89.76	5.12	3.74	0.01	98.63
(Troilite)	65.80	0.09	0.06	33.15	99.10
〃	62.19	0.09	0.63	36.40	99.31

Table 2. Basic Magnetic Properties of bulk, matrix, clast, metallic grains and extracted taenite of St. Séverin

Sample	I_S (emu/g)		I_R (emu/g)		H_C (Oe)		H_{RC} (Oe)	
	Before Heating	After Heating	Before Heating	After Heating	Before Heating	After Heating	Before Heating	After Heating
(Bulk)								
300K	2.80	3.95	0.50	0.021	520	9.5	1840	110
4.2K	3.85	5.10	0.68	0.125	430	39	2680	780
(Matrix)								
300K	7.4	10.2	1.43	0.17	590	35	1945	210
4.2K	8.2	11.7	1.64	0.21	575	38	2240	380
(Clast)								
300K	3.21	5.55	0.40	0.14	340	38	1310	300
4.2K	6.55	6.35	0.60	0.17	335	48	2110	350
(Metal)								
300K	142	124	25	0.20	860	3.5	895	47
4.2K	135	—	24	—	895	—	2300	—
(Tetrataenite)								
300K	127	128	23.5	0.40	765	3.5	1480	60
4.2K	—	144	—	0.70	—	7.0	—	38

Table 3. Basic magnetic properties of Appley Bridge (LL_6) and Tuxtuac (LL_5)

Sample	I_S (emu/g)		I_R (emu/g)		H_C (Oe)		H_{RC} (Oe)	
	Before Heating	After Heating	Before Heating	After Heating	Before Heating	After Heating	Before Heating	After Heating
(Appley Bridge)								
300K	1.73	2.42	0.121	0.031	160	14.5	470	70
4.2K	1.9	3.1	0.415	0.153	190	60	1210	3710
(Tuxtuac)								
300K	2.93	3.1	0.055	0.015	40	11	255	175
4.2K	3.6	4.45	0.176	0.128	90	60	3120	410

Table 4. Magnetic Transition Temperatures of Tetrataenite-rich meteorites

Meteorite	Tetrataenite (H_c) (°C)	Kamacite $(H^*_{\alpha\to\gamma})$ (°C)	Kamacite $(H^*_{\gamma\to\alpha})$ (°C)
Yamato 74160 (LL_7)	560	None	None
Appley Bridge (LL_6)	565	None	None
St. Séverin (LL_6) (Bulk)	565	780	665
ALH 77260 (L_3)	570	780	600-700
Tuxtuac (LL_5)	560	780	—
ALH 77219 (Mesosiderite)	560	760	630

REFERENCES

1. Clarke R.S.Jr. and Scott E.R.D., 1980,
Tetrataenite-ordered Fe Ni, a new mineral in meteorite.
American Mineral. 65, 624-630.

2. Crangle J. and Hallam G.C., 1963,
The magnetism of face-centred cubic and body-centred cubic iron nickel alloys.
Proc. Roy. Soc. London, A 272, 119-132.

3. Danon J., Scorzelli R.B. and Souza Azevedo I., 1979 a,
Iron-nickel superstructure in metal particles of chondrites.
Nature, 281, 469-473.

4. Danon J., Scorzelli R, Souza Azevedo I, Curvello W,
Albertsen J.F. and Knudsen J.M., 1979 b,
Iron-nickel 50-50 superstructure in the Santa Catharina meteorite. Nature, 227, 283-284.

5. Nagata T. and Funaki M., 1982,
Magnetic properties of tetrataenite-rich stony meteorites.
Proc. 7th Symp. Antar. Meteor., 222-250.

6. Nagata T. and Funaki M., 1983,
Magnetic analysis of an Antarctic mesosiderite, ALH-77219.

Antar Rec., 79, 1-10.

7. Wasilewski P.J., 1982,

Magnetic characterization of tetrataenite and its role in the magnetization. Lunar and Planetary Science XIII (Abstract), 843-844.